Sites and Regulation of Polyamine Catabolism in the Tobacco Plant. Correlations with Cell Division/Expansion, Cell Cycle Progression, and Vascular Development[1]

Konstantinos A. Paschalidis and Kalliopi A. Roubelakis-Angelakis*

Department of Biology, University of Crete, 71409 Heraklion Crete, Greece

We previously gave a picture of the homeostatic characteristics of polyamine (PA) biosynthesis and conjugation in tobacco (*Nicotiana tabacum*) plant organs during development. In this work, we present the sites and regulation of PA catabolism related to cell division/expansion, cell cycle progression, and vascular development in the tobacco plant. Diamine oxidase (DAO), PA oxidase (PAO), peroxidases (POXs), and putrescine *N*-methyltransferase expressions follow temporally and spatially discrete patterns in shoot apical cells, leaves (apical, peripheral, and central regions), acropetal and basipetal petiole regions, internodes, and young and old roots in developing plants. DAO and PAO produce hydrogen peroxide, a plant signal molecule and substrate for POXs. Gene expression and immunohistochemistry analyses reveal that amine oxidases in developing tobacco tissues precede and overlap with nascent nuclear DNA and also with POXs and lignification. In mature and old tissues, flow cytometry indicates that amine oxidase and POX activities, as well as *pao* gene and PAO protein levels, coincide with G2 nuclear phase and endoreduplication. In young versus the older roots, amine oxidases and POX expression decrease with parallel inhibition of G2 advance and endoreduplication, whereas putrescine *N*-methyltransferase dramatically increases. In both hypergeous and hypogeous tissues, DAO and PAO expression occurs in cells destined to undergo lignification, suggesting a different in situ localization. DNA synthesis early in development and the advance in cell cycle/endocycle are temporally and spatially related to PA catabolism and vascular development.

Polyamines (PAs) are abundant DNA- and RNA-binding organic cations. They have been correlated with specific roles in embryonic development (Kusunoki and Yasumasu, 1978), carcinogenesis and immune system functions (Seiler et al., 1998), defense (Schroder et al., 1998), antibiotic potency (Petropoulos et al., 2004), cell proliferation and apoptosis (for review, see Wallace et al., 2003; Janne et al., 2004), and in many biotic and abiotic stresses (Jokela et al., 1997; Kurepa et al., 1998; Perez-Amador et al., 2002; for review, see Bouchereau et al., 1999). Investigations on PA physiological functions have been focused mainly on changes in their levels and spectra, leaving the biological significance to be determined. Although genetic analyses have been conducted at the gene level (Paschalidis et al., 2001; Panicot et al., 2002; Tucker and Seymour, 2002; Cona et al., 2003; for review, see Janne et al., 2004), the available information on PA impact on plant development is limited. Furthermore, in plants, the potential relationship between PAs and hydrogen peroxide (H_2O_2) has so far not been examined in detail.

Reactive oxygen species (ROS) play a key role in cell wall expansion and growth, vascular differentiation, as well as lignin polymerization (Grant and Loake, 2000). We have thoroughly studied intra- and extracellular H_2O_2 and $O_2^{\cdot -}$ generation, accumulation, and scavenging in plant protoplasts (Siminis et al., 1994; de Marco and Roubelakis-Angelakis, 1996; Papadakis and Roubelakis-Angelakis, 1999, 2005; Papadakis et al., 2001). H_2O_2 generation in the apoplast can be ascribed to oxalate oxidases, $O_2^{\cdot -}$ dismutation (Papadakis et al., 2001), peroxidases (POXs; de Marco and Roubelakis-Angelakis, 1996), or amine oxidases (Laurenzi et al., 1999; Sebela et al., 2001; Rea et al., 2002; Papadakis and Roubelakis-Angelakis, 2005). H_2O_2 produced by the action of diamine oxidases (DAOs) and PA oxidases (PAOs) can be utilized by POX enzymes in wall-stiffening reactions during cell growth and differentiation (Wisniewski et al., 2000). In alkaloid producing plants, such as tobacco (*Nicotiana tabacum*), putrescine (Put), apart from serving as substrate for spermidine (Spd) biosynthesis or for oxidation (Bagni and Tassoni, 2001), is *N*-methylated by Put *N*-methyltransferase (PMT), which catalyzes the first committed steps in the biosynthesis of nicotine and tropane alkaloids (Sato et al., 2001).

A profile of PA fractions, their precursors, and their biosynthetic enzymes, along with correlations with age, cell division/expansion, and differentiation in the tobacco plant (cv Xanthi), has previously been presented (Paschalidis and Roubelakis-Angelakis, 2005). This work presents a detailed spatial and temporal profile of the expression of genes involved in PA

[1] This work was supported by the European Social Fund and National Resources.

* Corresponding author; e-mail poproube@biology.uoc.gr; fax 30−2810−394459 or 394408.

Article, publication date, and citation information can be found at www.plantphysiol.org/cgi/doi/10.1104/pp.105.063941.

catabolism, DAOs, PAOs, POXs, and PMT, related with DNA synthesis, cell cycle phases, cell division, and vascular development in tobacco. It also integrates whole-plant homeostasis of PAs giving insights into both anabolic and catabolic pathways during developmental processes. The PA catabolic network is regulated at different levels, spatially and temporally. DAO and PAO seem to act synergistically with POX in young vascular tissues with high DNA synthesis percentage and are mostly localized in the old vascular tissues with higher G2 phase and endoreduplication percentage; these cell types undergo lignification. However, PMT accumulates in young roots. Transcriptional, translational, and posttranslational levels of PAO show a consistent basipetal increase from leaf margins to petioles and internodes, which increase with plant age. The results support that amine oxidases and POXs are critical components in cell cycle/endocycle progression in vascular tissues of tobacco plants.

RESULTS

Amine Oxidases Increase Basipetally in Tobacco and Are Strongly Up-Regulated in Vascular Tissues

DAO and PAO activities increase basipetally both spatially and temporally at the hypergeous (aerial) parts of the tobacco plant (Fig. 1). Temporal basipetal increase occurs from the shoot apex to the plant base (with an exception of the leaf lamina regions). Spatial basipetal increase occurs from the apical and peripheral leaf regions to the (sequentially) central leaf areas, apical and basal petioles, and internodes. The increases of DAO and PAO activities in regions containing high percentage of vascular tissues (petioles and internodes) are observed early from the first to the second developmental stage and continue to peak at the oldest developmental stage (25th; Fig. 1). DAO and PAO are also highly expressed in root cells with a predominance for DAO in the older than in the younger ones.

POXs and PMT Exhibit Spatial and Temporal Correlation with Amine Oxidases in Hypergeous Tissues

POX and PMT specific activities also generally increase with age in hypergeous tobacco tissues (Fig. 1). They are also higher in internodes, lower in petioles, and even lower in leaves. Thus, a similar to amine oxidases distribution pattern is observed in POX and PMT expression in these tissues. POX activity and expression of amine oxidases are therefore associated mostly with tissues undergoing lignification and less with photosynthetic ones. We have previously detected an association of the three main PAs (Put, Spd, and spermine [Spm]) with thylakoid membranes and with various photosynthetic subcomplexes (Kotzabasis et al., 1993). At developmental stage 15, after full development, intense PMT expression is clearly present in the internode regions (Fig. 1). No significant expression is detected prior to this stage, independently of the tissue type analyzed, whereas in young roots PMT activity dramatically increases, indicating different PA catabolic processes in hypergeous and hypogeous tissues. This duality in PA catabolic pathways

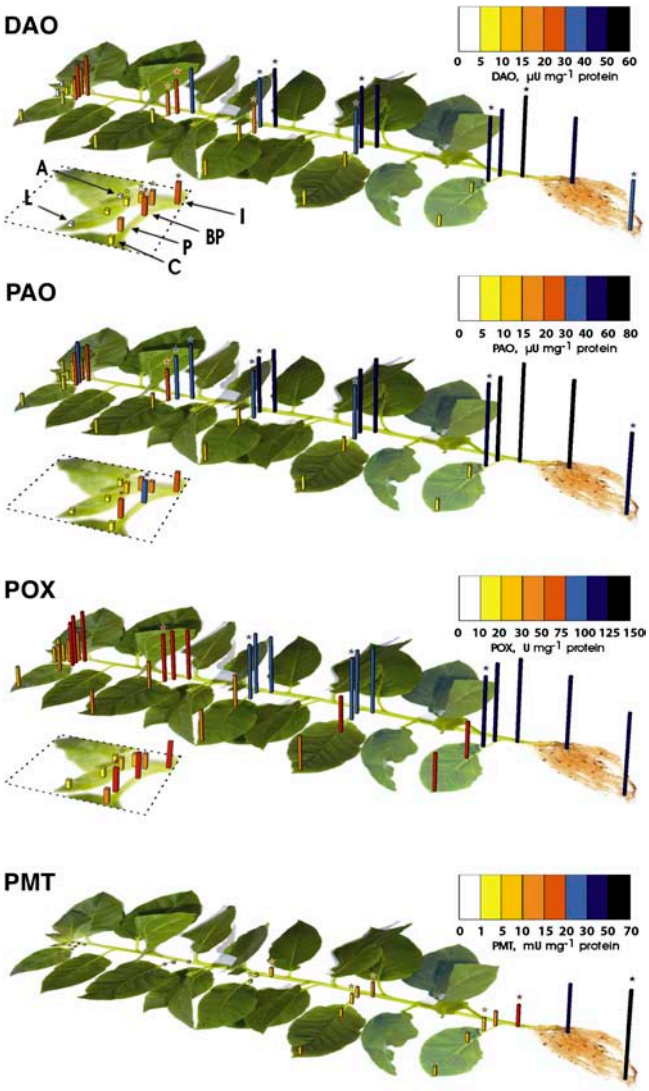

Figure 1. PMT, DAO, PAO, and POX specific activities in the soluble fractions from different parts of tobacco plants. The shoot apex (A), the first leaf, and part of the fifth leaf are also contained in the scale-ups of the figures (dotted lines). L, Apical and marginal leaf lamina; C, central lamina; P, acropetal petiole; BP, basipetal petiole; I, internode; R, primary root; r, secondary root. Data for L, C, P, BP, and I are depicted in the first, fifth, 10th, 15th, 20th, and 25th developmental stages (numbered from apex). Data for shoot apex, primary root, and secondary root are also depicted. DAO and PAO bars are depicted as μU mg^{-1} protein, PMT bars are depicted as mU mg^{-1} protein, whereas POX bars are depicted as U mg^{-1} protein. Asterisk-marked data regions indicate statistically significant differences ($P = 0.01$) when compared with the adjacent acropetal ones of the same developmental stage. In the first two developmental stages, asterisks are depicted in the scale-up parts, whereas asterisks on secondary roots indicate statistically significant differences from the primary roots.

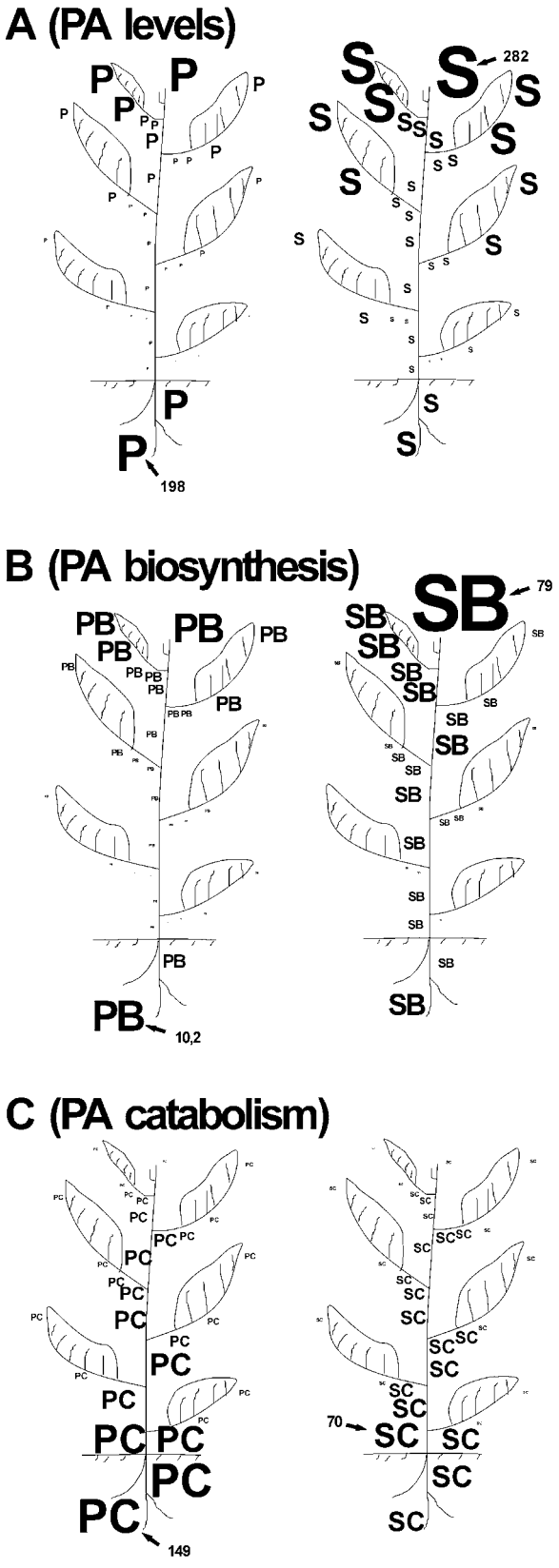

Figure 2. PAs as signal integrating developmental processes throughout the tobacco plant. PA levels (A) are estimated from the endogenous free titers (nmol g^{-1} fresh weight), whereas PA biosynthesis (B) and PA catabolism (C) are estimated from the enzyme specific activities in the soluble fractions. PA endogenous levels and specific activities are represented by magnitude levels depicted by the sizes of letters: P for Put levels, S for levels of higher PAs (Spd and Spm), PB for biosynthesis of Put, SB for biosynthesis of higher PAs, PC for catabolism of Put, and SC for catabolism of higher PAs. A, PA levels. Put levels are depicted as the free endogenous Put titers, whereas levels of higher PAs are depicted as the sum of free endogenous titers of Spd and Spm. B, Sites of PA biosynthesis. Biosynthesis of Put is depicted as a sum of ADC and ODC soluble activities. Biosynthesis of higher PAs is depicted as a sum of SPDS and SPMS activities. C, Sites of PA catabolism. Catabolism of Put is depicted as a sum of DAO and PMT soluble activities. Catabolism of higher PAs is depicted as PAO activities. Numbers 198 and 282 show (with arrows) the highest free PA endogenous titers (nmol g^{-1} fresh weight) depicted by the sizes of the biggest P and S, respectively (A). Numbers 10.2 and 79 show the highest soluble specific activity levels of the biosynthetic enzymes (in nmol [of the product measured] h^{-1} mg^{-1} protein) depicted by the sizes of the biggest PB and SB, respectively (B). Numbers 149 and 70 show the highest soluble specific activity levels of the catabolic enzymes (in mU [of both hot and cold products] mg^{-1} protein, 1 unit [U] = 1 μmol min^{-1}) depicted by the sizes of the biggest PC and SC, respectively (C). All the other sizes of the above letters are depicted proportionally to the respective biggest ones.

involves correlation of amine oxidases with PMT (for the production of nicotine alkaloids) and with POX (for the lignification, cell wall formation, and vascular differentiation). Furthermore, the estimation of Put catabolism via DAO and PMT reveals a complete picture for Put fate, throughout tobacco plant development.

Younger Roots Are the Highest Catabolic Sites of Put via PMT, and Old Shoot Internodes Are the Highest Catabolic Sites via DAO

The highest Put-catabolizing activity is observed in roots and the old hypergeous vascular tissues follow (Fig. 2C). The highest Put levels (Fig. 2A) and the highest Put-synthesizing capacity (Fig. 2B) are also observed in young roots. The high Put-catabolizing activity in young roots is mainly mediated by the catabolic activity of PMT, whereas DAO is responsible for the increased catabolic activity in older shoot internodes, which also exhibit the highest PAO activities (Fig. 1). A much lower rate of PA catabolism is present in young and expanding leaves and in the shoot apex (Fig. 2C). On the contrary, shoot apex is the site of the highest Spd + Spm levels (Fig. 2A) and the highest Spd + Spm biosynthetic capacity (Fig. 2B). Put catabolism in the oldest internodes and in the young roots is 15- and 16.5-fold higher than in the shoot apex, respectively, whereas the respective differences in Spd and Spm catabolism are 8- and 6.5-fold (Fig. 2C).

Basipetal Accumulation in Transcript and Protein of PAO

Northern- and western-blot analyses clearly show that transcript and protein for PAO accumulate during development in vascular tissues, reaching maximum levels in the oldest internodes and roots (Fig. 3, A and B). Also, they are generally higher in internodes, lower

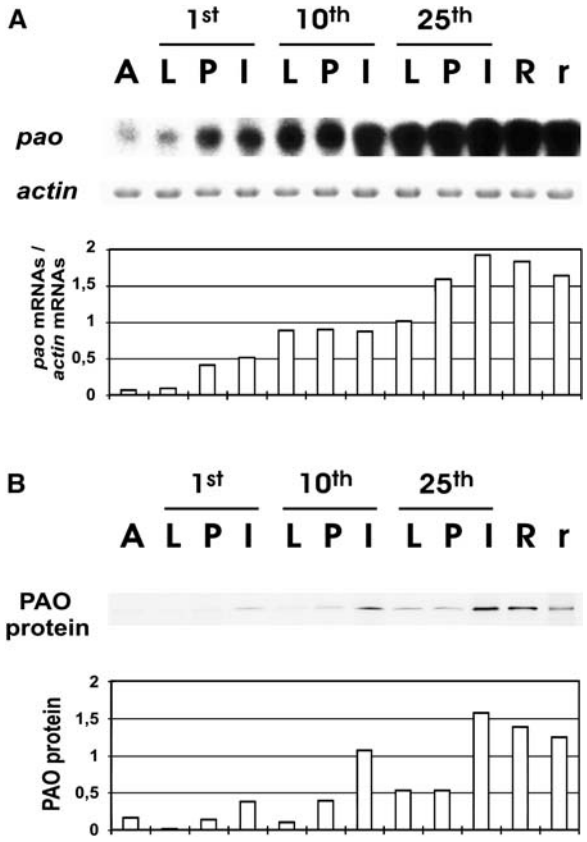

Figure 3. PAO expression in tobacco plants. A, RNA gel-blot analysis of the expression of the PAO gene and quantification of mRNA levels/actin mRNAs. B, Western-blot analysis of PAO and quantification of protein levels. Bands: A, Shoot apex; L, apical and leaf margin; P, acropetal petiole; I, internode; R, primary root; r, secondary root. Numbering started from shoot apex.

in petioles, and even lower in leaves, in agreement with the levels of specific activities (Fig. 1). During leaf growth, *pao* mRNA levels (Fig. 3A) generally present higher temporal differences than the specific activities (Fig. 1) and the protein levels (Fig. 3B). The transcripts of *pao* in young tissues exhibit also greater spatial differences than proteins and specific activities, whereas in the 10th and 25th developmental stages these differences are smaller (Fig. 3; data not shown). The results indicate that expression of *pao* is under strong spatial and temporal developmental control and suggest de novo synthesis during development.

The Activity Percentages of Amine Oxidases and POXs in the Soluble Fraction Relatively Decrease with Leaf Age, Whereas They Increase in the Particulate Fraction

In Figure 4, an overview of PA catabolism in young and old leaves and in young roots is shown. The specific activities of all DAO, PAO, POX, and PMT increase basipetally from young to old leaves with maximum in roots (Fig. 1). PA levels, on the contrary, decrease from young to old leaves, whereas roots also contain high PA titers (Fig. 4). The subcellular distribution of DAO and POX activities is also altered (Fig. 5). The relative contribution of the particulate fraction to the total enzyme activity increases significantly for DAO and POX (and PAO; data not shown) with

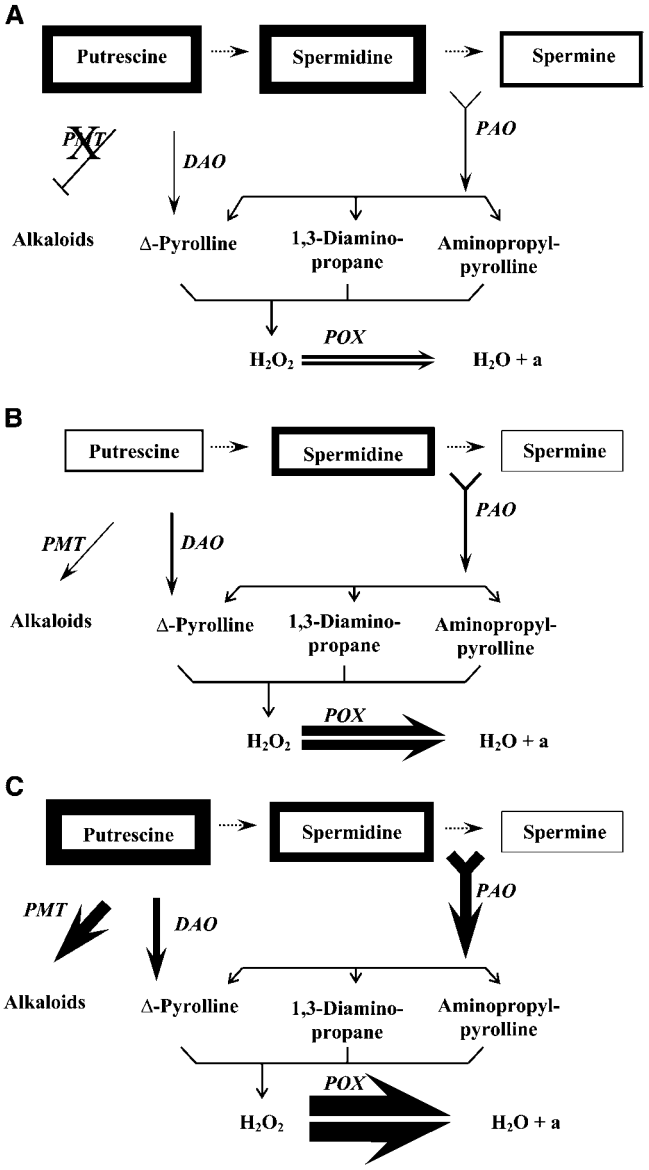

Figure 4. The tobacco PA biosynthetic pathway in the youngest leaf (A), oldest leaf (B), and young roots (C). The endogenous contents of free PAs are depicted by the thickness of their boxes, whereas the soluble specific activities of the catabolic enzymes (in italics) are depicted by the thickness of the corresponding arrows. In the youngest leaf (A), the contents of Put, Spd, and Spm (nmol mg^{-1} protein), depicted by the corresponding thicknesses of boxes, are 6.8, 7.8, and 2.5, respectively, whereas the specific activities of PMT, DAO, PAO, and POX (mU mg^{-1} protein), depicted by the corresponding thicknesses of arrows, are 0, 0.0059, 0.0074, and 25,000, respectively (white lines that separate POX arrows mean that cellular POX activities are much higher than the other enzyme specific activities). The thicknesses of boxes and arrows in B and C are depicted proportionally to the respective thicknesses in A. One unit (U) = 1 μmol min^{-1}. a, Any reductant.

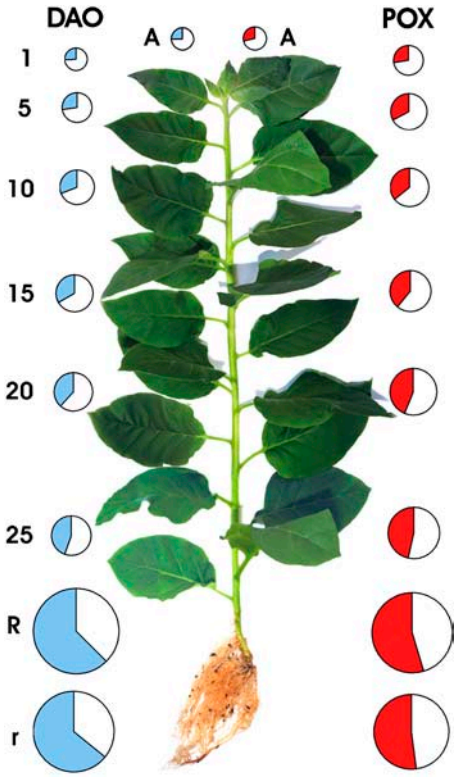

Figure 5. DAO and POX specific activities in the soluble and particulate fractions in tobacco plants. The area of the circles designates the relative DAO (left) and POX (right) values in different organs of the plant. White parts of the circles designate the activities of soluble enzymes. Blue and red parts designate the activities of particulate DAO and POX, respectively. A, Shoot apex; 1, 5, 10, 15, 20, and 25 leaves from apex; R, primary root; r, secondary root. The size of the DAO circle in the apical meristem (A) corresponds to 6.1 μU mg^{-1} protein and includes the white (soluble) and blue (particulate) portions corresponding to 4.6 and 1.4 μU mg^{-1} protein, respectively. The size of the POX circle in the apical meristem corresponds to 24 U mg^{-1} protein and includes the white (soluble) and red (particulate) portions corresponding to 17 and 7 U mg^{-1} protein, respectively. The sizes of circles (and the respective white and blue or white and red portions) in the other plant organs are proportionally depicted.

maximum values in roots and minimum in young leaves and shoot apex, whereas the respective soluble fraction decreases (Fig. 5).

Tobacco Young Cells Have More Nuclei in the S and G1 Phases But Correlate Negatively with the G2 Advance

Growth during plant development is predominantly governed by the combined activities of cell division and cell elongation (Raz and Koornneef, 2001). PAs have been proposed to affect nuclear stages in yeast (Chattopadhyay et al., 2002), whereas in mammals Orn decarboxylase (ODC) translation peaks twice during the cell cycle, at the G1/S transition and at G2/M (Pyronnet et al., 2000). Taking into consideration the above, together with our finding that PA synthesis and distribution are correlated with cell division regions in tobacco (Paschalidis and Roubelakis-Angelakis, 2005), we hypothesized that PAs may be involved in cell cycling, or in the cellular decision to place the wall either toward the outside leading to cell expansion or to the cell plate via the phragmoplast. Thus, in accordance with this hypothesis, cells expressing high levels of PA synthesis would either be binucleate or contain nuclei in the S or G2/M phases. Therefore, we measured the nuclear phases of cells in all tobacco tissues by flow cytometry in order to correlate them with PA homeostasis; the fifth and 25th developmental stages, along with roots, are depicted in Figure 6. Generally, all regions of the tobacco plants have an increasing gradient percentage of nuclei in the G2 phase from the shoot apex to the base, whereas the G1 phases decrease. These differences mostly occur in the vascular tissues (petioles and internodes; Fig. 6). It is noteworthy that neither mitotic nor binucleate cells were easily observed in old leaf sections (data not shown), so the second peak in flow cytometry represents cells arrested in the G2 phase. The percentages of nuclei in the G2 phase are in agreement with the results reported by Galbraith et al. (1983). The S phase nuclei, as measured from the values of the DNA content between the G1 and G2 nuclear stages, also decrease with age of the explant (Fig. 6). Immunochemical analysis showed that the newly synthesized DNA in nuclei (after incorporation of 5-bromo-2-deoxyuridine [BrdU]), versus total nuclear DNA (after staining with 4′,6-diamidino-2-phenylindole [DAPI]), further confirms these findings (Fig. 7). Cross sections and protoplasts taken from old leaves contained a single, but distinctly larger, DAPI-stained nucleus, consistent with the higher percentage of nuclei in the G2 phase shown by flow cytometry. The measurement of DNA content by flow cytometry was straightforward for tobacco nuclei, but the preparation of isolated nuclei from old root tissues was more difficult, which is reflected by the respective noise in the dot plot (Fig. 6).

Endoreduplication in Tobacco Is Limited in Old Vascular Tissues and Coincides with Amine Oxidase Expression

In Figure 6, the 2C (G1), 4C (G2), and 8C ploidy levels of cells are presented. A spatial and temporal shift in the DNA content at the C-value level is observed in the tobacco plant. With increasing developmental stage, the frequency of 2C cells in all explants decreases and the frequencies of 4C cells simultaneously increase. Furthermore, endoreduplication coincides with age (and cell size) increase (Fig. 6). 8C cells were observed mostly in old petioles and internodes (8% and 10%, respectively, in the oldest); 16C cells were rarely observed and could not be depicted in histograms. In hypergeous tissues, high percentage of nuclei in G2 phase (Fig. 6) temporally and spatially correlate with high amine oxidase and

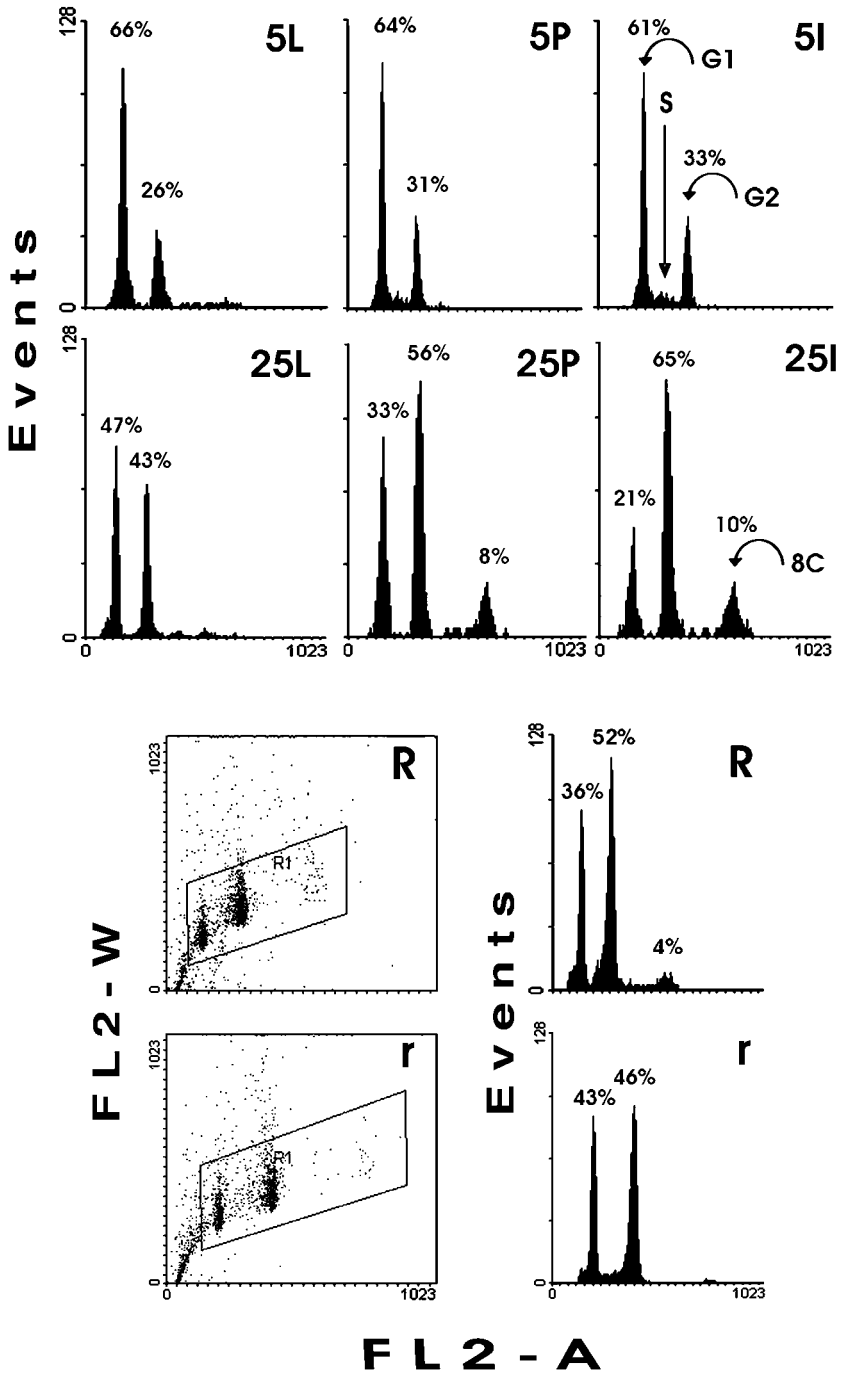

Figure 6. The frequency distribution of DNA content (FL2-A) versus nuclear number (events) histograms in tobacco nuclei stained with propidium iodide. The FACScan immunocytometry system has been used to identify subpopulations of 2C (G1), S, 4C (G2), and 8C nuclei, differing in DNA content. 5L and 25L, Apical regions (and margins) of the fifth and 25th leaves (from apex), respectively; 5P and 25P, apical regions of the fifth and 25th petioles, respectively; 5I and 25I, fifth and 25th internodes, respectively. R, Primary root; r, secondary root. The dot blots represent cytograms of the area fluorescence versus width in primary and secondary roots. Only dots within the regions displayed are included in the respective histogram analyses.

POX expression, as well as with PMT levels (Fig. 1). In old hypergeous tissues, these enzymes also correlate with endoreduplication.

DNA Synthesis Is Mostly Localized in Young Vascular Cells and Correlates with the Onset of Amine Oxidation in Tobacco

In the fifth developmental stage, the S phase nuclei percentages were higher in petiole and internode tissues versus leaf lamina (Fig. 6) and in central versus peripheral tip lamina (data not shown). The higher DNA synthesis in these tissues was also confirmed by BrdU labeling of DNA gel blots (Fig. 7A) and tissue sections (Fig. 7, I–L). DNA synthesis is strongly localized in vascular (mostly phloem and companion) cells (Fig. 7, I, K, and L), where both Spd synthesis (Paschalidis and Roubelakis-Angelakis, 2005) and catabolism via amine oxidation (Fig. 1) mostly occur, and was first observed in the vascular bundles of the first internode (Fig. 7, C and F, leaf traces). In young roots, DNA synthesis was high in cells of the endodermis

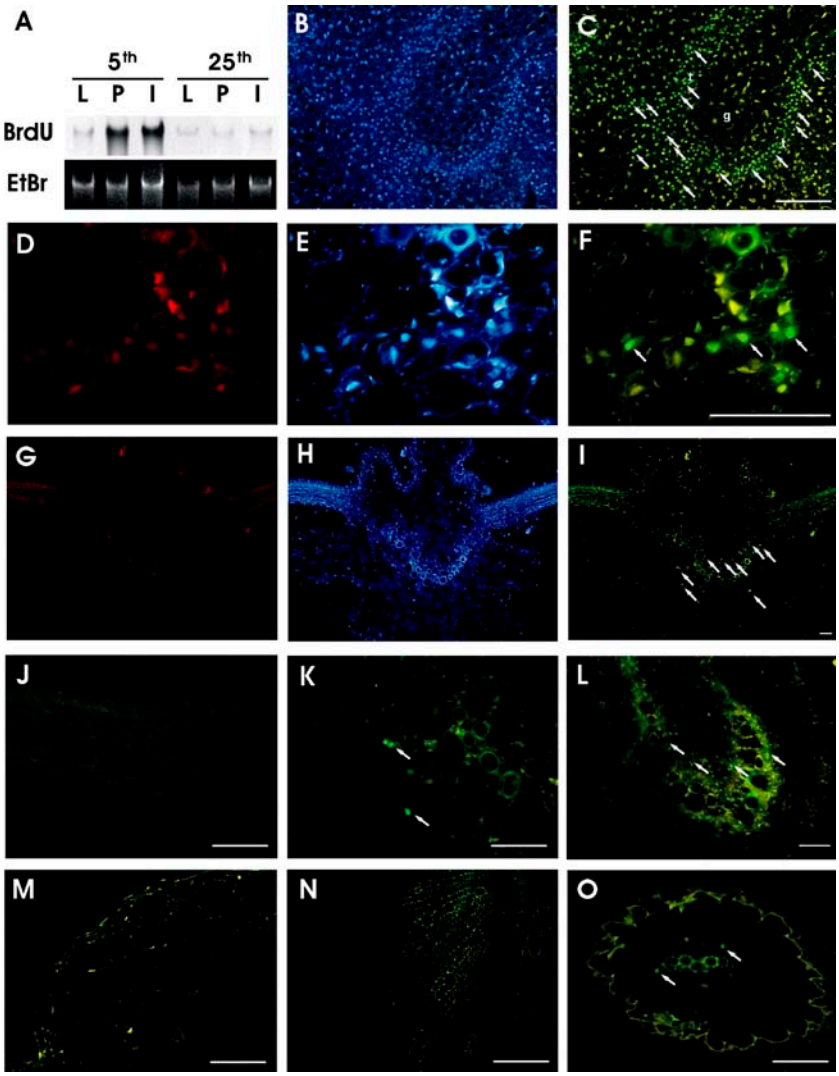

Figure 7. BrdU incorporation into DNA. Tobacco tissues were incubated with 100 μM BrdU for 24 h. A, DNA gel-blot analysis. L, Apical and marginal leaf lamina; P, acropetal petiole; I, internode; EtBr, ethidium bromide. B, E, and H, Chromatin staining with fluorochrome DAPI (blue). D and G, Autofluorescence (red). Tissues with high chlorophyll content have a strong autofluorescence. C, F, and I to O, BrdU labeling. B and C, Transverse section of the first internode. Arrows indicate some of the BrdU-labeled nuclei in the leaf trace. Leaf trace (t) has numerous nuclei with nascent DNA, whereas leaf gap (g) presents very few nuclei in the S phase. D to F, Close-ups of C. G to I, Transverse section of midrib at base of lamina of the fifth leaf, with the two lamina sides. Arrows indicate some BrdU labeling in vascular cells. J, Close-up of lamina section of I. K, Close-up of midrib section of I. L, Cross section of the fifth internode. Arrows indicate BrdU labeling in vascular cells. M, BrdU labeling in a cross section of an old internode. Only cell wall autofluorescence is observed. N, BrdU labeling in a cross section of primary root, where cell walls have a strong autofluorescence. O, BrdU labeling in a cross section of secondary root. Scale bars = 100 μm.

(Fig. 7O), whereas in old roots (Fig. 7N), lamina tissues of the fifth to 25th leaves (Fig. 7J; data not shown), and mature petioles and internodes (Fig. 7M; data not shown), nuclei with nascent DNA were rarely detected.

Autofluorescence (red; Fig. 7, D and G) is high, but this is not an unusual phenomenon (Lucretti et al., 1999). However, only the green-colored nuclei are strongly stained with BrdU. Fixed plant cells presented higher nonspecific binding of the antibody than isolated nuclei (data not shown). Higher than 2 M HCl concentration for DNA denaturation, or heating denaturation, drastically reduced autofluorescence but resulted in cell damage and significant cell loss, especially in young tissues. Furthermore, since DAPI intercalates into double-stranded DNA, nuclear DNA must be denatured only partially to leave sufficient double-stranded DNA for DAPI binding. BrdU incorporation in tissues with no nascent DNA may also reflect an initial response of the plant to the presence of BrdU.

DISCUSSION

The specific activities of the enzymes in PA catabolism, PMT, DAO, PAO, as well as POX increase basipetally in the leaf central and basal, petiolar, and internode regions throughout development (Fig. 1). Although amine oxidase enzyme activities and PAO protein levels moderately increase with ontogenic stage, mRNA levels dramatically increase with age (more than 10-fold from the youngest to the oldest leaf), suggesting that changes in *pao* expression are mainly regulated at the transcriptional level.

Auxin gradients are largely associated with cell division and differentiation (Chen et al., 2001; Hay et al., 2004), and ethylene, an antagonist of PAs (Janne et al., 2004), directs cell division in the apical hook (Raz and Koornneef, 2001). Auxin levels, which temporally decrease with age (Chen et al., 2001), are negatively correlated with the age-mediated induction of amine oxidases expression in the vascular tissues of tobacco. PAO is down-regulated by auxin in maize (*Zea mays*)

mesocotyl (Cona et al., 2003). Thus, the temporal modulation of *pao* gene expression might also be down-regulated by auxin in tobacco tissues. Furthermore, cells at the tip and marginal regions of the youngest tobacco leaf, which have the highest capacity for auxin-induced growth (Jones et al., 1998) and the highest auxin levels (Chen et al., 2001), also have the highest titers of all PA fractions and the highest biosynthetic activities (Paschalidis and Roubelakis-Angelakis, 2005) but have the lowest DAO, PAO, and POX specific activities, suggesting also a spatial regulation. However, in the older leaves, where the cell division pattern, together with the profile of auxin contents, is reverse increasing basipetally from peripheral to petiole regions (Chen et al., 2001), the specific activities of PA catabolic enzymes continue to follow the same basipetally increasing gradient. Auxins are also referred to cause a transient increase in free PAs and in Arg decarboxylase (ADC) and ODC activities (Alabadí et al., 1996) and an up-regulation in expression of ODC and Spd synthase (SPDS) genes (Alabadí and Carbonell, 1998, 1999) during early parthenocarpic fruit development. Furthermore, the jasmonate-induced up-regulation of PA biosynthetic genes (Biondi et al., 2001; Goossens et al., 2003) is differently modified by the presence/absence of exogenously supplied auxins and cytokinins in the medium (Biondi et al., 2003).

Age-induced increase in *pao* expression in the tobacco plant could be the result of a complex regulation. Different transcription factors could modulate *pao* gene transcription. Age-mediated reduction of auxin supply from the shoot apex into the differentiated tissues could disable putative auxin-responsive repressors, like ARF transcription factors (Ulmasov et al., 1997). Furthermore, increased photosynthetic efficiency coincident with age increase until the middle-aged leaves could stimulate light-responsive transactivators (Oyama et al., 1997). PAO activity (Fig. 1) and mRNA levels (Fig. 3) increase 2-fold and 9-fold, respectively, from the first to the 10th tobacco leaf (from apex) and remain fairly constant thereafter.

ODC is generally associated with cells undergoing cell division (Acosta et al., 2005) and ADC with cells undergoing cell expansion correlating with increased Put synthesis (Perez-Amador and Carbonell, 1995). In transgenic carrot (*Daucus carota*) and poplar (*Populus* spp.) cells, these pathways also work independently (Andersen et al., 1998; Bhatnagar et al., 2001). On the other hand, inhibition of PA biosynthesis resulted in cell cycle arrest at the G1 phase, suggesting the involvement of PAs in DNA synthesis (Chattopadhyay et al., 2002). In both hypergeous and hypogeous parts of the tobacco plant, an increasing gradient percentage on nuclei in the G2 phase is observed from young to old tissues, whereas the S and G1 phases concomitantly decrease (Figs. 6 and 7). Put levels and Put biosynthetic enzymes, as well as Spd + Spm levels and their biosynthetic enzymes, also decrease from young to old tissues in both hypergeous and hypogeous parts (Fig. 2, A and B). In *Chlamydomonas reinhardtii* synchronized cultures, an increase in Put and Spd levels and in ODC activity was measured during the transition from the cell enlargement to the cell division phase preceding the increase in aphidicholine-sensitive DNA polymerase activity (S phase; Theiss et al., 2002). Application of inhibitors of *S*-adenosylmethionine decarboxylase and SPDS in these cultures prevented cell divisions (Theiss et al., 2002), while *Spds* mutant Arabidopsis (*Arabidopsis thaliana*) seeds have embryos that do not develop beyond the torpedo stage (Imai et al., 2004), indicating that synthesis of Spd has an essential role in cell division. Expression of *spds* is higher in young vascular tissues that have higher cell division percentages, as compared with the respective lamina (Paschalidis and Roubelakis-Angelakis, 2005). This spatial SPDS pattern follows the S phase patterns in these tissues (Figs. 6 and 7) and is also correlated with the respective G2 (Fig. 6). The temporal analyses suggest that within the first hour after tobacco leaf formation, PAs are degraded by amine oxidases in the vascular tissues. In the fifth developmental stage, the SPDS expression pattern coincides to the amine oxidases and to the POX ones (Fig. 1) in regions also with high percentage of nuclei in the S and G2 phases (Figs. 6 and 7). In older tissues, amine oxidases coincide with POX in regions with higher G2, over the G1, cell cycle stage, and in endoreduplicated cells (Fig. 6). Endoreduplication is a different cell cycle mode in which cells undergo iterative DNA replications without any subsequent mitosis and cytokinesis (Inzé, 2005). This cell cycle mode is frequently observed in some plants, but the level of ploidy varies between species and tissues (Sugimoto-Shirasu and Roberts, 2003) and between cells of different morphogenic competence (Ochatt et al., 2000). In tobacco, a relationship between vascular tissue development, cell elongation, and the overall transition from 2C to 4C DNA content is revealed, whereas cells with 8C DNA content were found mainly in explants from mature petioles and internodes (Fig. 6). Endoreduplication was not observed in leaf lamina tissues (Fig. 6), so endoreduplication-related changes in tobacco may be a requisite only for vascular cells such as petiolar and internodal cells.

In animal cells, increased Spd and Spm synthesis is often accompanied by increased catabolic breakdown of these compounds through induction of Spm acetyltransferase and PAO activities (Cohen, 1998), whereas a direct correlation between the biosynthesis and oxidation of PAs has been known for many years in plants (Torrigiani et al., 1987; 1989). This study's results support the view that both anabolic and catabolic enzymes play a role in the regulation of PA levels during cell cycle and cell division/expansion processes in tobacco. On the other hand, PA catabolism may also act as a way to generate H_2O_2, which is considered as an active secondary messenger (Vandenabeele et al., 2003). DAO and POX (Fig. 5) enzyme activities are present in both the soluble and particulate fractions of almost all tobacco cells,

suggesting a role in the synthesis of H_2O_2 both intraprotoplasmically and wall localized. PAO has also been suggested to play an intraprotoplasmic and wall localized role in the synthesis of H_2O_2 in maize (Cona et al., 2003). A wall-localized increased production of H_2O_2 is needed to sustain in muro diferulate cross-bridge formation and lignification (de Marco and Roubelakis-Angelakis, 1996).

During vascular differentiation, lignin precursors are polymerized into lignin by a process that requires H_2O_2 and cell wall-bound POXs or a laccase-like activity (de Marco and Roubelakis-Angelakis, 1996). Enzymes that may be responsible for H_2O_2 generation include a POX-catalyzed oxidation of NADH produced by a cell wall-bound laccase or NADPH oxidase (Papadakis et al., 2001), DAO (Rea et al., 2002), and PAO (Cona et al., 2003). The strong up-regulation of DAO and PAO in vascular tissues and their direct correlation with POX (Figs. 1 and 4), as well as with the advance in cell cycle/endocycle during vascular development (Fig. 6), could make amine oxidases an attractive candidate for a role in the generation of H_2O_2 for cell wall-bound POX-mediated protein cross-linking and/or lignification in tobacco. On the other hand, PMT directly uses Put for the production of nicotine alkaloids in root and in old hypergeous tobacco tissues.

Our previous results on the distribution of PA conjugation and synthesis and on the understanding of the engagement of ROS in the biogenesis and modification of cell wall structure, as well as this work concerning the spatial and temporal regulation of the expression of PA catabolic enzymes in tobacco, allow envisioning a new scenario of the molecular events regulating cell wall extension and differentiation. Fast extension growth of tobacco leaf is known to be sustained by auxin, mostly transported from the shoot apex (Chen et al., 2001), with concomitant basipetal decrease in PA levels and synthesis. The cytoplasmic localization of DAO and PAO may account for the intraprotoplasmic production of H_2O_2 for polymer cross-linking in the secretory pathway. Vascular development results in the induction of cell cycle/endocycle progression and DAO, PAO, and POX expression, with a great increase of their abundance in the cell walls. This event is probably linked to the physiological requirement of higher production of H_2O_2 via amine oxidases in the apoplast to drive POX-catalyzed cross-linking and lignification to complete cell wall stiffening and stimulate endoreduplication.

In conclusion, this developmentally dictated expression analysis correlates PA catabolism with PA synthesis and conjugation, DNA synthesis and cell division/expansion, advance in cell cycle/endoreduplication, cell wall cross-linking/lignification, and nicotine alkaloid production in tobacco. Further studies, including PA transport and the generation of ROS during the above processes, along with studies of mutant or transgenic lines with altered PA metabolism, altered H_2O_2 levels, or other, will be of help to better understand these mechanisms in plant development.

MATERIALS AND METHODS

Plant Material

Six- to 8-week-old tobacco (*Nicotiana tabacum* L. cv Xanthi) plants were used. Leaf and petiole explants were numbered from shoot apex and divided in tip and leaf margin, leaf center, acropetal or apical petiole, and basipetal or basal petiole. Shoot apex, primary or main root, and secondary or newly formed root explants were also removed.

Protein Extraction and Determination

Total proteins were extracted as already described (Primikirios and Roubelakis-Angelakis, 2001). After centrifugation of the homogenates, the supernatants (soluble fractions) were desalted in Bio-gel P-6 spin columns (Bio-Rad, Hercules, CA). The pellets (cell walls, nucleus, plastids, and mitochondria) were redissolved in half-strength extraction buffer, supplemented with 1 M NaCl, centrifuged, and gave the particulate fractions. Proteins were determined by the method of Lowry et al. (1951) and by visualization on gels.

PA Analysis and Enzyme Assays

PA fractions were determined according to Kotzabasis et al. (1993), with an HP 1100 HPLC (Hewlett-Packard, Waldbronn, Germany).

PMT was assayed by measuring the Put decrease and the formation of methylputrescine. The assay mixture contained 3 mM Put, 2 mM *S*-adenosylmethionine, 100 mM Tris-HCl buffer, pH 9.0, and the enzyme in a total volume of 200 μL. The reaction was performed at 37°C for 1 h and stopped by the addition of 200 μL of 65 mM borate-KOH buffer, pH 10.5, followed by addition of 1 mL of 2 N NaOH and 10 μL benzoylchloride. The benzoyl-PAs were separated in a C-18 narrow-bore column with an HP 1100 HPLC system. One unit (U) of PMT activity represents the amount of enzyme catalyzing the decrease of 1 μmol of Put/min.

DAO and PAO enzyme activities were estimated by a modification of the radiometric method of Biondi et al. (2001), using [1,4-^{14}C]Put and [1,4-^{14}C]Spd (Amersham, Buckinghamshire, UK; specific activities 4.37 GBq mmol^{-1}; Santanen and Simola, 1994) as labeled substrates. The assay mixture contained 0.5 mL of the extract, 1 mM unlabeled Put or Spd, and 3.7 KBq of [1,4-^{14}C]Put or [1,4-^{14}C]Spd. After incubation on a shaker at 37°C for 60 min, the reaction was terminated by adding 150 μL of saturated sodium carbonate (Bhatnagar et al., 2002). Labeled Δ^1-pyrroline was extracted immediately in 1 mL toluene. The 0.5-mL aliquots were placed in scintillation liquid (0.5% [w/v] 2,5-diphenyloxazole and 0.05% [w/v] 1,4-bis[5-phenyloxazoyl]benzene in toluene) and counted in an LS 6000SE (Beckman, Fullerton, CA) scintillation counter. One unit of enzyme (U) represents the amount of enzyme catalyzing the formation of 1 μmol of Δ^1-[^{14}C]pyrroline/min. A spectrophotometric assay was also used for DAO and PAO enzyme activities, according to Federico et al. (1985), but the extraction buffer for PAO consisted of 0.1 M K-phosphate, pH 6.5, 10 μM pyridoxal phosphate, 2 mM dithiothreitol, and the reaction mixture contained the enzyme, 12 μL Spd 0.1 M, and up to 1 mL 0.1 M K-phosphate, pH 6.5.

POX activity was determined photometrically at 460 nm (Church and Galston, 1988). One unit of enzyme (U) represents the amount catalyzing the oxidation of 1 μmol of *o*-dianisidine/min. POX activity was also determined following tetraguaiacol formation at 470 nm in a reaction volume of 1 mL containing 0.1 M potassium phosphate buffer, pH 7.0, 5 mM guaiacol, and 5 mM H_2O_2.

Western Blotting, RNA Extraction, and Northern Blotting

Proteins were electrophoretically resolved, transferred to membranes and incubated with an anti-MPAO polyclonal antibody (Angelini et al., 1995).

Total RNA was extracted as already described (Logemann et al., 1987), quantified by spectroscopy and ethidium staining, electroforesed, and transferred to Gene Screen membranes (Primikirios and Roubelakis-Angelakis, 1999). Membranes were screened with a *pao* cDNA obtained from tobacco shoot. Two degenerate oligonucleotide primers corresponding to two

conserved regions in the aligned sequences of maize (*Zea mays*; Tavladoraki et al., 1998) and Arabidopsis (*Arabidopsis thaliana*; At5g13700) PAO proteins, sense 5′-ACNGARGAYGGNTCNGTNTAYGAR-3′ and antisense 5′-RTANCCNCCRTGNACRTANCC-3′, were used to obtain a 579-bp product, which was cloned and sequenced.

Isolation of Nuclei and Flow Cytometric Analysis

Tissues were chopped in the presence of propidium iodide and RNase (Galbraith et al., 1983) to final concentrations 100 μg mL^{-1} and 10 μg mL^{-1}, respectively. Stained nuclei were analyzed by flow cytometry (FACScan, Becton-Dickinson Immunocytometry, Franklin Lakes, NJ) with a 488-nm light source from a 15-mW argon ion laser. Chicken red blood cells were used as internal standard and for instrument alignment.

Immunolocalization and DNA Gel-Blot Analysis of BrdU Incorporation

Tobacco explants were placed in 0.5× Hoagland solution (Hoagland and Arnon, 1950) containing 100 μM BrdU (Calbiochem, La Jolla, CA) for 24 h. Ten-micrometer paraffin-embedded sections were cut using a Vibratome 1000 (Technical Products International, St. Louis). For the DNA gel-blot analysis, DNA was electrophoresed, stained with ethidium bromide, and blotted to nitrocellulose membranes (Sambrook et al., 1989).

Sections and membranes were blocked in phosphate-buffered saline-bovine serum albumin and incubated with anti-BrdU monoclonal antibody (Becton-Dickinson, 1/100 for sections and 1/1,000 for membranes). Sections were then incubated with goat anti-mouse IgG conjugated with Alexa 488 and membranes with a goat anti-mouse IgG horseradish POX conjugate (Molecular Probes, Eugene, OR). Images were obtained using a Nikon Eclipse E800 fluorescence microscope, a Sony DXC-950 camera system (Tokyo), and Scion Image analysis software (Scion, Frederick, MD).

Statistical Analysis and Preparation of Figures

All experiments were carried out three times with similar results and included a minimum of three replicates/samples. Statistical analysis of data concerning enzyme activities and mRNA/rRNAs ratios was performed with one-way ANOVA to determine whether statistically significant differences occurred among groups being tested. Bands were quantified with Kodak Digital Science 1D Image Analysis Software (Eastman Kodak, Rochester, NY). Upon request, all novel materials described in this publication will be made available in a timely manner for noncommercial research purposes.

ACKNOWLEDGMENTS

The authors are grateful to Dr. P. Tavladoraki (University Roma Tre, Italy) for the anti-PAO polyclonal antibody, and Prof. D. Kalpaxis (University of Patras, Greece) for some of the labeled PA substrates. The authors thank T. Makatounakis (Institute of Molecular Biology and Biotechnology/Foundation for Research and Technology-Hellas) and L. Panagis (University of Crete, Greece) for help in FACScan analysis and BrdU labeling, respectively.

Received April 7, 2005; revised April 28, 2005; accepted April 30, 2005; published July 22, 2005.

LITERATURE CITED

Acosta C, Pérez-Amador MA, Carbonell J, Granell A (2005) The two ways to produce putrescine in tomato are cell-specific during normal development. Plant Sci **168:** 1053–1057

Alabadí D, Agüero MS, Pérez-Amador MA, Carbonell J (1996) Arginase, arginine decarboxylase, ornithine decarboxylase, and polyamines in tomato ovaries: changes in unpollinated ovaries and parthenocarpic fruits induced by auxin or gibberellin. Plant Physiol **112:** 1237–1244

Alabadí D, Carbonell J (1998) Expression of ornithine decarboxylase is transiently increased by pollination, 2,4-dichlorophenoxyacetic acid, and giberellic acid in tomato ovaries. Plant Physiol **118:** 323–328

Alabadí D, Carbonell J (1999) Molecular cloning and characterization of a tomato (*Lycopersicon esculentum* Mill.) spermidine synthase cDNA (accession no. AJ006414) (PGR 99–103). Plant Physiol **120:** 935

Andersen SE, Bastola DR, Minocha SC (1998) Metabolism of polyamines in transgenic cells of carrot expressing a mouse ornithine decarboxylase cDNA. Plant Physiol **116:** 299–307

Angelini R, Federico R, Bonfante P (1995) Maize polyamine oxidase: antibody production and ultrastructural localization. J Plant Physiol **145:** 686–692

Bagni N, Tassoni A (2001) Biosynthesis, oxidation and conjugation of aliphatic polyamines in higher plants. Amino Acids **20:** 301–317

Bhatnagar P, Glasheen BM, Bains SK, Long SL, Minocha R, Walter C, Minocha SC (2001) Transgenic manipulation of the metabolism of polyamines in poplar cells. Plant Physiol **125:** 2139–2153

Bhatnagar P, Minocha R, Minocha SC (2002) Genetic manipulation of the metabolism of polyamines in poplar cells: the regulation of putrescine catabolism. Plant Physiol **128:** 1455–1469

Biondi S, Scaramagli S, Capitani F, Altamura MM, Torrigiani P (2001) Methyl jasmonate upregulates biosynthetic gene expression, oxidation and conjugation of polyamines, and inhibits shoot formation in tobacco thin layers. J Exp Bot **52:** 231–242

Biondi S, Scoccianti V, Scaramagli S, Ziosi V, Torrigiani P (2003) Auxin and cytokinin modify methyl jasmonate effects on polyamine metabolism and ethylene biosynthesis in tobacco leaf discs. Plant Sci **165:** 95–101

Bouchereau A, Aziz A, Larher F, Martin-Tangui J (1999) Polyamines and environmental challenges: recent development. Plant Sci **140:** 103–125

Chattopadhyay MK, Tabor CW, Tabor H (2002) Absolute requirement of spermidine for growth and cell cycle progression of fission yeast (Schizosaccharomyces pombe). Proc Natl Acad Sci USA **99:** 10330–10334

Chen J, Shimomura S, Sitbon F, Sandberg G, Jones AM (2001) The role of auxin-binding protein 1 in the expansion of tobacco leaf cells. Plant J **28:** 607–617

Church DL, Galston AW (1988) 4-Coumarate coenzyme of A ligase and isoperoxidase expression in Zinnia mesophyll cells induced to differentiate into tracheary elements. Plant Physiol **88:** 679–684

Cohen SS (1998) A Guide to the Polyamines. Oxford University Press, New York

Cona A, Cenci F, Cervelli M, Fedrico R, Mariottini P, Moreno S, Angelini R (2003) Polyamine oxidase, a hydrogen peroxide-producing enzyme, is up-regulated by light and down-regulated by auxin in the outer tissues of the maize mesocotyl. Plant Physiol **131:** 803–813

de Marco A, Roubelakis-Angelakis KA (1996) The complexity of enzymic control of hydrogen peroxide concentration may affect the regeneration potential of plant protoplasts. Plant Physiol **110:** 137–145

Federico R, Angelini R, Cesta A, Pini C (1985) Determination of diamine oxidase in lentil seedlings by enzymic activity and immunoreactivity. Plant Physiol **79:** 62–64

Galbraith DW, Harkins KR, Maddox JM, Ayres NM, Sharma DP, Firoozabady E (1983) Rapid flow cytometric analysis of the cell cycle in intact plant tissues. Science **220:** 1049–1051

Goossens A, Häkkinen ST, Laakso I, Seppänen-Laakso T, Biondi S, De Sutter V, Lammertyn F, Nuutila AM, Söderlund H, Zabeau M, et al (2003) A functional genomics approach toward the understanding of secondary metabolism in plant cells. Proc Natl Acad Sci USA **100:** 8595–8600

Grant JJ, Loake GJ (2000) Role of reactive oxygen intermediates and cognate redox signalling in disease resistance. Plant Physiol **124:** 21–29

Hay A, Barkoulas M, Tsiantis M (2004) PINning down the connections: transcription factors and hormones in leaf morphogenesis. Curr Opin Plant Biol **7:** 575–581

Hoagland DR, Arnon DI (1950) The water culture method for growing plants without soil. Calif Agric Ext Serv Circ **347:** 1–32

Imai A, Matsuyama T, Hanzawa Y, Akiyama T, Tamaoki M, Saji H, Shirano Y, Kato T, Hayashi H, Shibata D, et al (2004) Spermidine synthase genes are essential for survival of Arabidopsis. Plant Physiol **135:** 1565–1573

Inzé D (2005) Green light for the cell cycle. EMBO J **24:** 657–662

Janne J, Alhonen L, Pietila M, Keinanen TA (2004) Genetic approaches to the cellular functions of polyamines in mammals. Eur J Biochem **271:** 877–894

Jokela A, Sarjala T, Kaunisto S, Huttunen S (1997) Effects of foliar potassium concentration on morphology, ultrastructure and polyamine concentrations of Scots pine needles. Tree Physiol **17:** 677–685

Jones AM, Im KH, Savka MA, Wu MJ, DeWitt NG, Shillito R, Binns AN (1998) Auxin-dependent cell expansion mediated overexpressed auxin-binding protein 1. Science **282:** 1114–1117

Kotzabasis K, Fotinou C, Roubelakis-Angelakis KA, Ghanotakis D (1993) Polyamines in the photosynthetic apparatus: photosystem II highly resolved subcomplexes are enriched in spermine. Photosynth Res **38:** 83–88

Kurepa J, Smalle J, Van Montagu M, Inzé D (1998) Polyamines and paraquat toxicity in Arabidopsis thaliana. Plant Cell Physiol **39:** 987–992

Kusunoki S, Yasumasu I (1978) Inhibitory effect of alpha-hydrazinoornithine on egg cleavage in sea urchin eggs. Dev Biol **67:** 336–345

Laurenzi M, Rea G, Federico R, Tavladoraki P, Angelini R (1999) De-etiolation causes a phytochrome-mediated increase of polyamine oxidase expression in outer tissues of the maize mesocotyl: role in the photomodulation of growth and cell wall differentiation. Planta **208:** 146–154

Logemann J, Schell J, Willmitzer L (1987) Improved method for the isolation of RNA from plant tissues. Anal Biochem **163:** 16–20

Lowry OH, Rosebrough NJ, Farr AL, Randall RJ (1951) Protein measurement with the Folin phenol reagent. J Biol Chem **193:** 265–275

Lucretti S, Nardi L, Nisini PT, Moretti F, Gualberti G, Dolezel J (1999) Bivariate flow cytometry DNA/BrdUrd analysis of plant cell cycle. Methods Cell Sci **21:** 155–166

Ochatt SJ, Mousset-Déclas C, Rancillac M (2000) Fertile pea plants regenerate from protoplasts when calluses have not undergone endoreduplication. Plant Sci **156:** 177–183

Oyama T, Shimura Y, Okada K (1997) The Arabidopsis HY5 gene encodes a bZIP protein that regulates stimulus-induced development of root and hypocotyls. Genes Dev **11:** 2983–2995

Panicot M, Minguet EG, Ferrando A, Alcázar R, Blázquez MA, Carbonell J, Altabella T, Koncz C, Tiburcio AF (2002) A polyamine metabolon involving aminopropyl transferase complexes in Arabidopsis. Plant Cell **14:** 2539–2551

Papadakis AK, Roubelakis-Angelakis KA (1999) The generation of active oxygen species differs in Nicotiana and Vitis plant protoplasts. Plant Physiol **121:** 197–245

Papadakis AK, Roubelakis-Angelakis KA (2005) Polyamines inhibit NADPH oxidase-mediated superoxide generation and putrescine prevents programmed cell death induced by polyamine oxidase-generated hydrogen peroxide. Planta **220:** 826–837

Papadakis AK, Siminis CI, Roubelakis-Angelakis KA (2001) Reduced activity of antioxidant machinery is correlated with suppression of totipotency in plant protoplasts. Plant Physiol **126:** 434–444

Paschalidis KA, Aziz A, Geny L, Primikirios NI, Roubelakis-Angelakis KA (2001) Polyamines in grapevine. *In* KA Roubelakis-Angelakis, ed, Molecular Biology and Biotechnology of the Grapevine. Kluwer Academic Publishers, Dordrecht, The Netherlands, pp 109–152

Paschalidis KA, Roubelakis-Angelakis KA (2005) Spatial and temporal distribution of polyamine levels and polyamine anabolism in different organs/tissues of the tobacco plant: correlations with age, cell division/expansion, and differentiation. Plant Physiol **138:** 142–152

Perez-Amador MA, Carbonell J (1995) Arginine decarboxylase and putrescine oxidase in ovaries of *P. sativum*. Plant Physiol **107:** 865–872

Perez-Amador MA, Leon J, Green PJ, Carbonell J (2002) Induction of the arginine decarboxylase ADC2 gene provides evidence for the involvement of polyamines in the wound response in Arabidopsis. Plant Physiol **130:** 1454–1463

Petropoulos AD, Xaplanteri MA, Dinos GP, Wilson DN, Kalpaxis DL (2004) Polyamines affect diversely the antibiotic potency. J Biol Chem **279:** 26518–26525

Primikirios NI, Roubelakis-Angelakis KA (1999) Cloning and expression of an arginine decarboxylase cDNA from Vitis vinifera L. cell-suspension cultures. Planta **208:** 574–582

Primikirios NI, Roubelakis-Angelakis KA (2001) Indications for post-translational regulation of Vitis vinifera L. arginine decarboxylase. Plant Mol Biol **45:** 669–678

Pyronnet S, Pradayrol L, Sonenberg N (2000) A cell cycle-dependent internal ribosome entry site. Mol Cell **5:** 607–616

Raz V, Koornneef M (2001) Cell division activity during apical hook development. Plant Physiol **125:** 219–226

Rea G, Metoui O, Infantino A, Federico R, Angelini R (2002) Copper amine oxidase expression in defense responses to wounding and *Ascochyta rabiei* invasion. Plant Physiol **128:** 865–875

Sambrook J, Fritsh EF, Maniatis T (1989) Molecular cloning: A Laboratory Manual, Ed 2. Cold Spring Harbor Laboratory Press, Cold Spring Harbor, NY

Santanen A, Simola LK (1994) Catabolism of putrescine and spermidine in embryogenic and non-embryogenic callus lines of *Picea abies*. Physiol Plant **90:** 125–129

Sato F, Hashimoto T, Hachiya A, Tamura K, Choi K, Morishige T, Fujimoto H, Yamada Y (2001) Metabolic engineering of plant alkaloid biosynthesis. Proc Natl Acad Sci USA **98:** 367–372

Schroder FC, Farmer JJ, Attygale AB, Smedley SR, Eisner T, Meinwald J (1998) Combinatorial chemistry in insects: a library of defensive macrocyclic polyamines. Science **281:** 428–431

Sebela M, Radova A, Angelini R, Tavladoraki P, Frebort II, Pec P (2001) FAD-containing polyamine oxidases: a timely challenge for researchers in biochemistry and physiology of plants. Plant Sci **160:** 197–207

Seiler N, Atanassov CL, Raul F (1998) Polyamine metabolism as target for cancer chemoprevention. Int J Oncol **13:** 993–1006

Siminis CI, Kanellis AK, Roubelakis-Angelakis KA (1994) Catalase is differentially expressed in dividing and nondividing protoplasts. Plant Physiol **105:** 1375–1383

Sugimoto-Shirasu K, Roberts K (2003) 'Big it up': endoreduplication and cell-size control in plants. Curr Opin Plant Biol **6:** 1–10

Tavladoraki P, Schinina ME, Cecconi F, Di Agostino S, Manera F, Rea G, Mariottini P, Federico R, Angelini R (1998) Maize polyamine oxidase: primary structure from protein and cDNA sequencing. FEBS Lett **426:** 62–66

Theiss C, Bohley P, Voigt J (2002) Regulation by polyamines of ornithine decarboxylase activity and cell division in the unicellular green alga *Chlamydomonas reinhardtii*. Plant Physiol **128:** 1470–1479

Torrigiani P, Serafini-Fracassini D, Bagni N (1987) Polyamine biosynthesis and effect of dicyclohexylamine during the cell cycle of *Helianthus tuberosus* tuber. Plant Physiol **84:** 148–152

Torrigiani P, Serafini-Fracassini D, Fara A (1989) Diamine oxidase activity in different physiological stages of *Helianthus tuberosus* tuber. Plant Physiol **89:** 69–73

Tucker G, Seymour G (2002) Tomato plants engineered with increased levels of polyamines show delayed ripening and increased levels of the antioxidant lycopene. Nat Biotechnol **20:** 558–560

Ulmasov T, Hagen G, Guilfoyle TJ (1997) ARF1, a transcription factor that binds auxin response elements. Science **276:** 1865–1868

Vandenabeele S, Van Der Kelen K, Dat J, Gadjev I, Boonefaes T, Morsa S, Rottiers P, Slooten L, Van Montagu M, Zabeau M, et al (2003) A comprehensive analysis of hydrogen peroxide-induced gene expression in tobacco. Proc Natl Acad Sci USA **100:** 16113–16118

Wallace HM, Fraser AV, Hughes A (2003) A perspective of polyamine metabolism. Biochem J **376:** 1–14

Wisniewski JP, Rathbun EA, Knox JP, Brewin NJ (2000) Involvement of diamine oxidase and peroxidase in insolubilization of the extracellular matrix: implications for pea nodule initiation by Rhizobium leguminosarum. Mol Plant Microbe Interact **13:** 413–420